Cell Metabolism, Volume *29*

Supplemental Information

The Mouse Microbiome Is Required for Sex-Specific Diurnal Rhythms of Gene Expression and Metabolism

Benjamin D. Weger, Cédric Gobet, Jake Yeung, Eva Martin, Sonia Jimenez, Bertrand Betrisey, Francis Foata, Bernard Berger, Aurélie Balvay, Anne Foussier, Aline Charpagne, Brigitte Boizet-Bonhoure, Chieh Jason Chou, Felix Naef, and Frédéric Gachon

Supplemental Figures and Legends

Figure S1: GF mice show tissue-specific alteration in their transcriptome profiles and mildly altered peripheral circadian clocks, related to Fig. 1

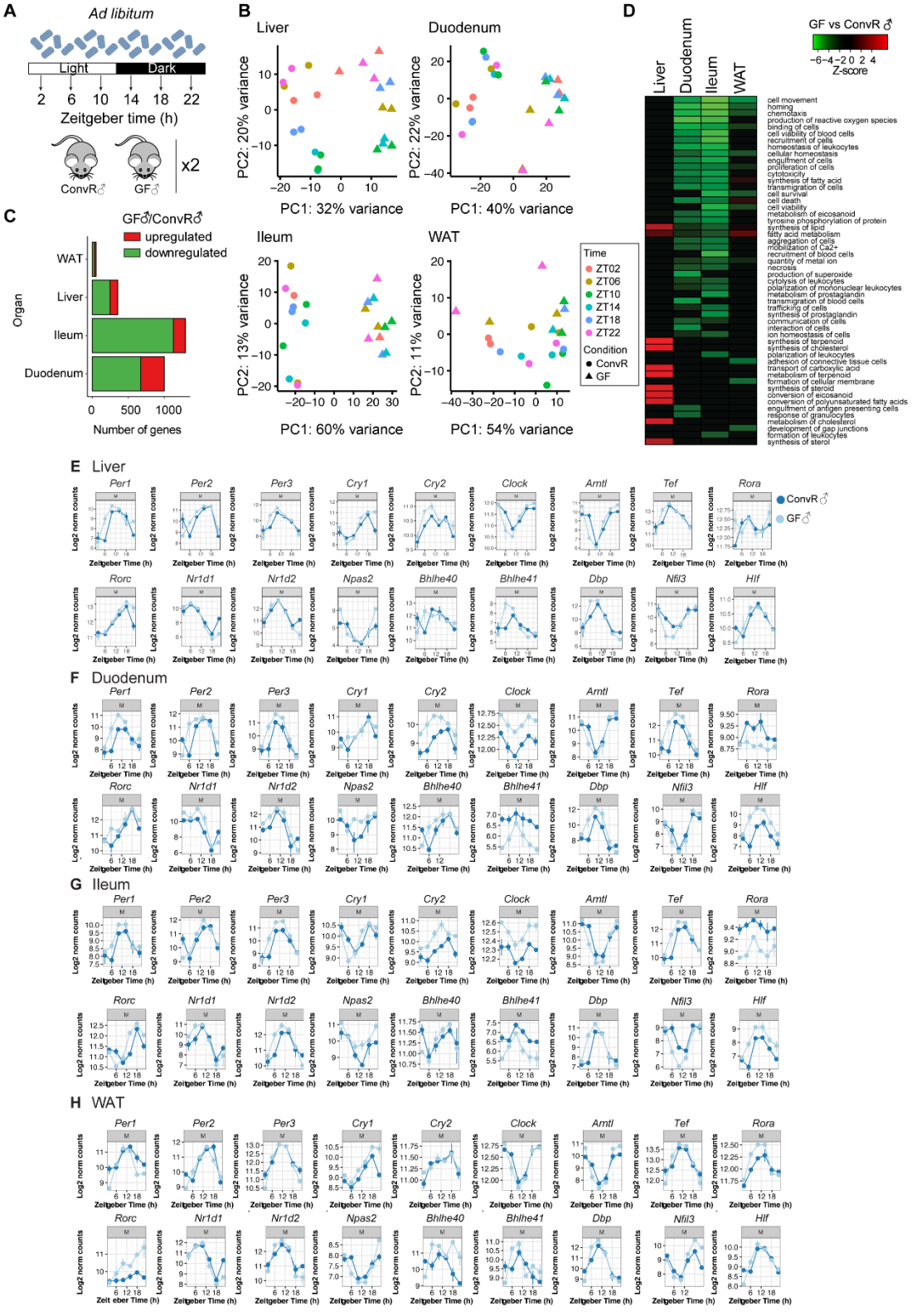

A. Sampling schedule of the transcriptome profiling of ConvR and GF male (♂) mice. Animals were fed *ad libitum*, kept under a 12 h light (white bar) and 12 h dark (black bar) regimen, and sacrificed every 4 h.
B. PCA of RNA-Seq expression data are shown from the indicated organs in male ConvR and GF mice.
C. Number of up- and down-regulated genes (log2 fold change ≥ 1, adjusted p-value ≤ 0.01) of GF male mice in the indicated organs.
D. Ingenuity Pathway Analysis (IPA) of the differentially expressed genes in GF mice shows the top significant biological functions in the indicated organs. Biological functions that are expected to be activated and repressed are associated with a positive (red) and negative (green) Z-score, respectively.
E-H. Clock gene expression in male ConvR (ConvR♂, blue) and GF (GF♂, light blue) in liver (E) duodenum (F), ileum (G), and WAT (H) measured by RNA-Seq. Error bars represent SEM.

Figure S2: Male GF mice show a feminization in gene expression in a broad range of conditions, related to Fig 2

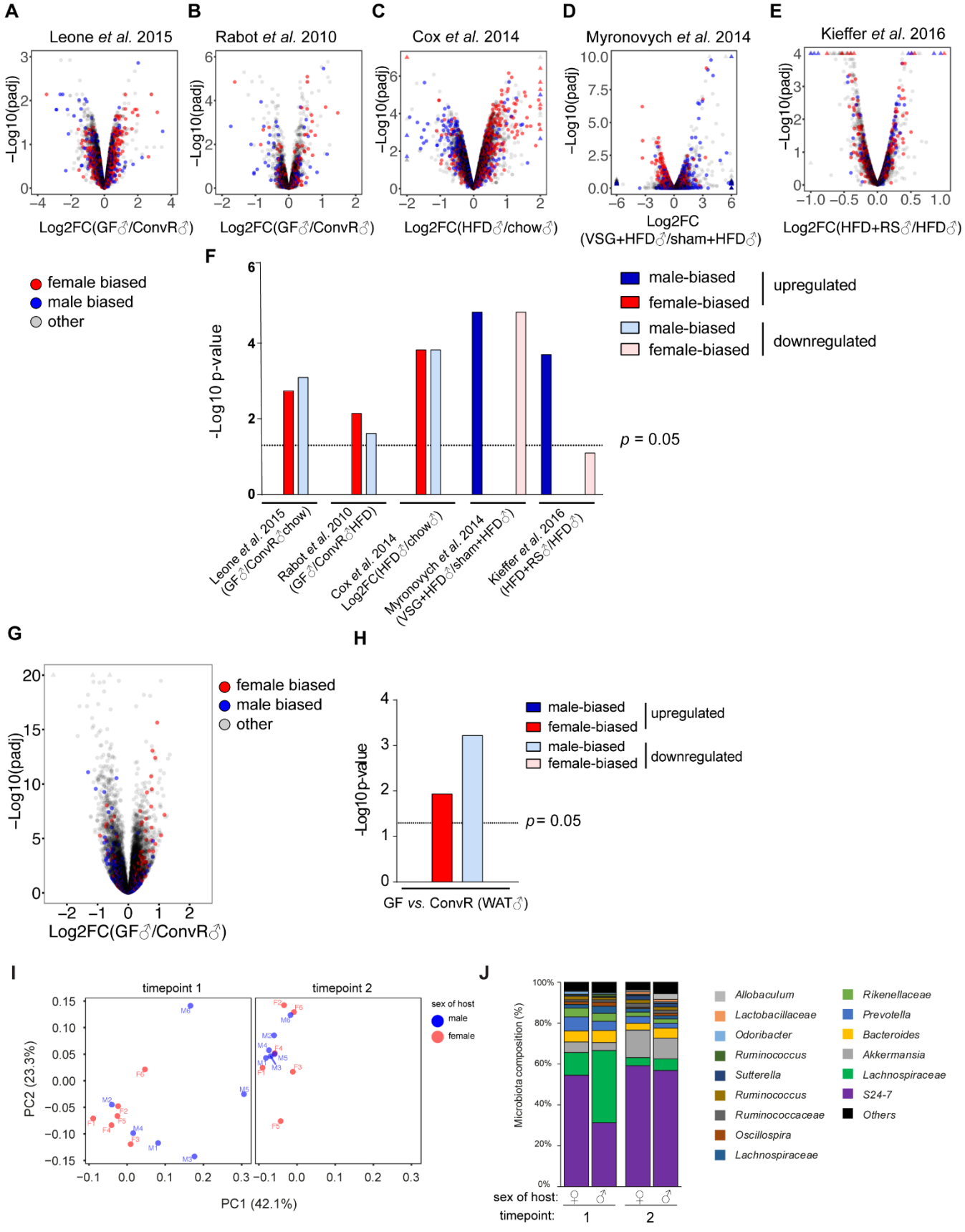

A. Analysis of published liver gene expression in GF male mice (Leone et al., 2015). Change in gene expression and the according p-values in male GF (GF♂) *vs* ConvR (ConvR♂) presented as a volcano plot. Sex biased genes are indicated in red (for female biased) and blue (for male biased), whereas sex independent genes in this study are shown in gray (others).
B. Liver sexually dimorphic gene expression in GF male mice under HFD (Rabot et al., 2010).
C-E. Effects of HFD on sex-specific gene expression on the liver transcriptome and the impact of conditions known to modify the gut microbiota. Changes in hepatic gene expression (log2FC) and adjusted p-values in HFD fed animals (Cox et al., 2014) (C), VSG treated animals on HFD (Myronovych et al., 2014) (D) and resistant starch fed animals on HFD (Kieffer et al., 2016) (E) presented as a volcano plot.
F. Graph depicts the associated p-values for significant enrichment of female-biased and male-biased genes in the subset of up and down regulated genes in the different conditions shown in panel A-E.
G, H. Feminization of gene expression in WAT. (G) Volcano-plot of gene expression in GF♂ mice *vs* ConvR♂. (H) Adjusted p-value for the enrichment of male- and female-biased genes in GF♂.
I. PCoA plots of the weighted UniFrac distances (16S rRNA genes sequencing) between male and female ConvR mice upon arrival from the supplier (timepoint 1) and after 2 weeks of daily interchanging bedding (timepoint 2).
J. Relative abundances of predominant bacterial families in the fecal samples of male and female ConvR mice at the indicated timepoints.

Figure S3: Sex-specific transcription factor, GH signaling in GF mice, related to Fig 3 and Fig 4

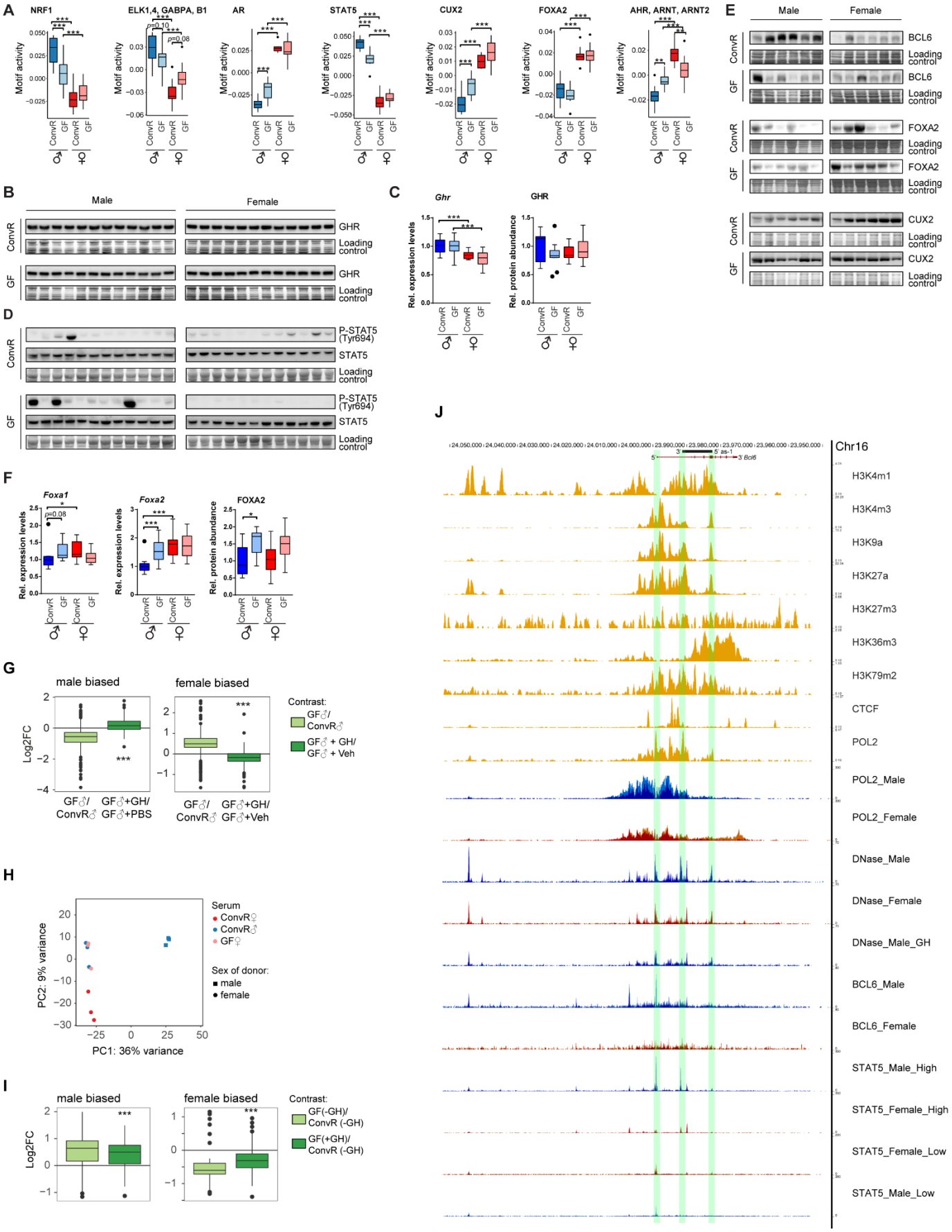

A. Predicted motif activity of indicated transcription factors in the liver of male (♂) and female (♀) ConvR and GF mice.
B, C. GHR exhibits stable mRNA and protein abundance in liver extracts across all conditions: male (♂) and female (♀) ConvR and GF mice. (B) Protein levels were measured by Western blot on total extracts. (C) Hepatic mRNA levels of *Ghr* and protein quantification of the Western blot on male and female ConvR and GF mice. Boxplots represent 12 biological replicates for each condition.
D. Western blot analysis of P-STAT5 (Tyr694) and total STAT5 protein levels in liver extracts from male and female ConvR and GF male mice.
E. Hepatic protein levels of the sex-specific TFs BCL6, FOXA2 and CUX2 in ConvR♂, ConvR♀, GF♂ and GF♀. All loading controls of the presented Western blots are Naphtol blue-black staining of the membrane.
F. Hepatic mRNA levels of *Foxa1* and *Foxa2* and protein quantification of FOXA2 CUX2 in ConvR♂, ConvR♀, GF♂ and GF♀.
G. Log2 fold change of hepatic differentially expressed male (left) or female biased (right) genes (GF♂ vs ConvR♂) are blunted in GH injected GF males. GH rescues sexually dimorphic gene expression.
H. PCA score plots of Total RNA-Seq samples of female and male primary hepatocytes (sex of donor) under indicated serum treatment (Serum). Female hepatocytes treated with serum derived from ConvR♂ and GF♀ show an overlap in PC2.
I. Log2 fold change of differentially expressed male (left) or female biased (right) genes (GF♂ vs ConvR♂) are attenuated under a tonic treatment of GH. The differences of differentially expressed sex biased genes between GF and ConvR male mice are strongly attenuated by GH injections.
J. Hepatic genomic landscape of the *Bcl6* locus. ChIP-Seq profiles of histone modification, RNA Polymerase II (POL2) occupation, insulator protein CTCF and transcription factor binding sites at the *Bcl6* gene locus. Sense and AS transcripts (*as-1* and *as-2*) are indicated at the top of the figure. The upper data tracks (yellow) show POL2, CTCF and chromatin modification marks from the Encode project (Consortium, 2012; Shen et al., 2012). Active promoters are usually characterized by the presence of Pol2, H3K4me3, H3K9a and H3K27a. Active enhancers correlate often with an absence of H3K4me3 and H3K4me1 and the presence of H3K27a. H3K36me3 and H3K79m2 are usually found in actively transcribed regions. H3K9me3 and H3K27me3 mark transcriptionally silent regions in the genome. CTCF traces are a marker for insulators. Histone marks for promoter activity localize with the putative TSS of *as-2*. The lower tracks depict sex specific (blue = male, red = female) DNAse I hypersensitivity and ChIP-Seq data that was retrieved from several sources (See Methods). DNAse I hypersensitive sites under chronic GH treatment mimicking female GH secretion (DNAse_male_GH), BCL6 sites, STAT5 sites at trough (Stat5_Male_Low, Stat5_Female_Low) and peak (Stat5_Male_High) levels for GH, Pol2 occupancy (Pol2_Male and Pol2_Female) and DNAse I hypersensitivity revealed two male specific BCL6 sites upstream and one at the TSS of the sense *Bcl6* transcript, in addition to one male specific STAT5 site at the TSS. An additional male specific STAT5 site localizes with the 3'end of the *as-1* transcript.
*, $p \leq 0.05$, **, $p \leq 0.01$, ***, $p \leq 0.001$. All boxplots are Tukey boxplots and represent at least 6 biological replicates.

Figure S4 Sex-specific transcriptional and metabolic rhythmicity is attenuated in the liver of GF mice, related to Fig. 5

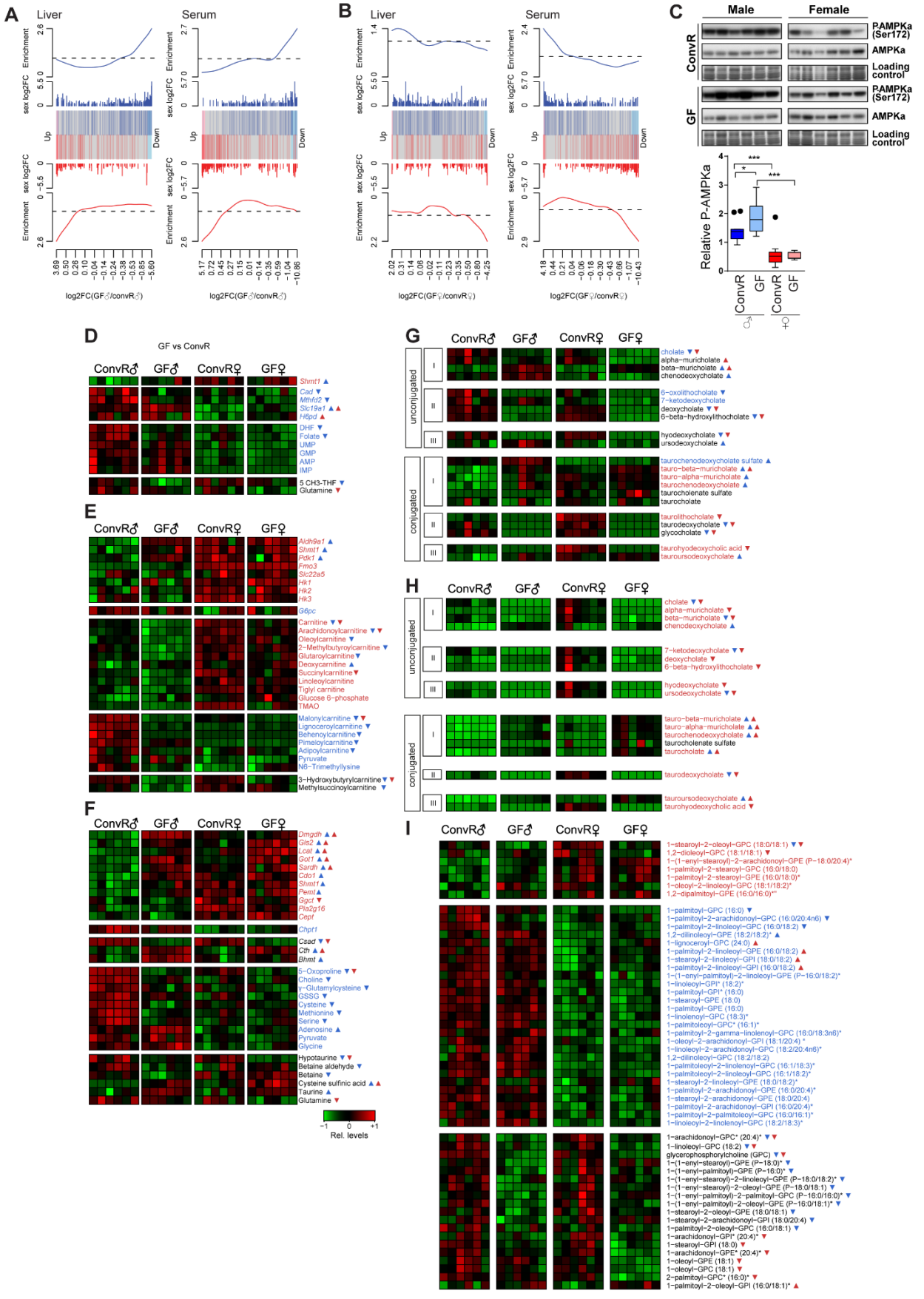

A, B. Barcode plots for metabolites in liver (left) and serum (right) depicting the enrichment of male-biased and female-biased metabolites. Metabolites are ordered by t-statistics from most up to most downregulated metabolite in GF male (GF♂ vs ConvR♂) (A) and female (GF♀ vs ConvR♀) (B). Log2 fold change (sex log2FC) of sex-biased metabolites of ConvR♂ vs ConvR♀ mice are represented as vertical blue (male-biased) and red bars (female-biased). Relative enrichment is plotted as red and blue lines for male and female biased metabolites, respectively.

C. Phosphorylation of AMPKα and total AMPKα protein expression was measured by Western blot on total extracts in ConvR♂/♀ and GF♂/♀ animals. Naphtol blue-black stained membranes served as a loading control. Tukey boxplot represents the densitometry measurements of P-AMPKα (Ser172) of 6 independent biological replicates per condition. Values were normalized to loading and total AMPKα levels. *, $p \leq 0.05$, ***, $p \leq 0.001$.

D-F. Heatmaps for folate, purine and pyrimidine metabolism (D), Glycolysis and fatty acid oxidation (E) and the metabolic network of glutathione (GSH, methionine, PL and BA) (F) depict relative mRNA (upper part) and metabolite levels (lower part) in ConvR♂/♀ and GF♂/♀ mice. Genes and metabolites are classified according to their sex bias and changes in the absence of microbiota. Colored metabolite name indicates sex-unbiased (black), male-biased (blue) and female-biased (red) metabolite levels. Triangle following metabolite name indicates the direction of significant change in GF♂ (blue) and GF♀ (red) mice in comparison to their ConvR counterpart.

G, H. Heatmaps of BA levels in liver (G) and serum (H) of ConvR♂/♀ and GF♂/♀ mice. BA are categorized according to their classification as unconjugated and conjugated primary (I), secondary (II) and tertiary forms (III).

I. Heatmaps of PL level in liver of ConvR♂/♀ and GF♂/♀ mice.

Figure S5: Sexually dimorphic hepatic gene expression is altered in GF mice, related to Fig 5

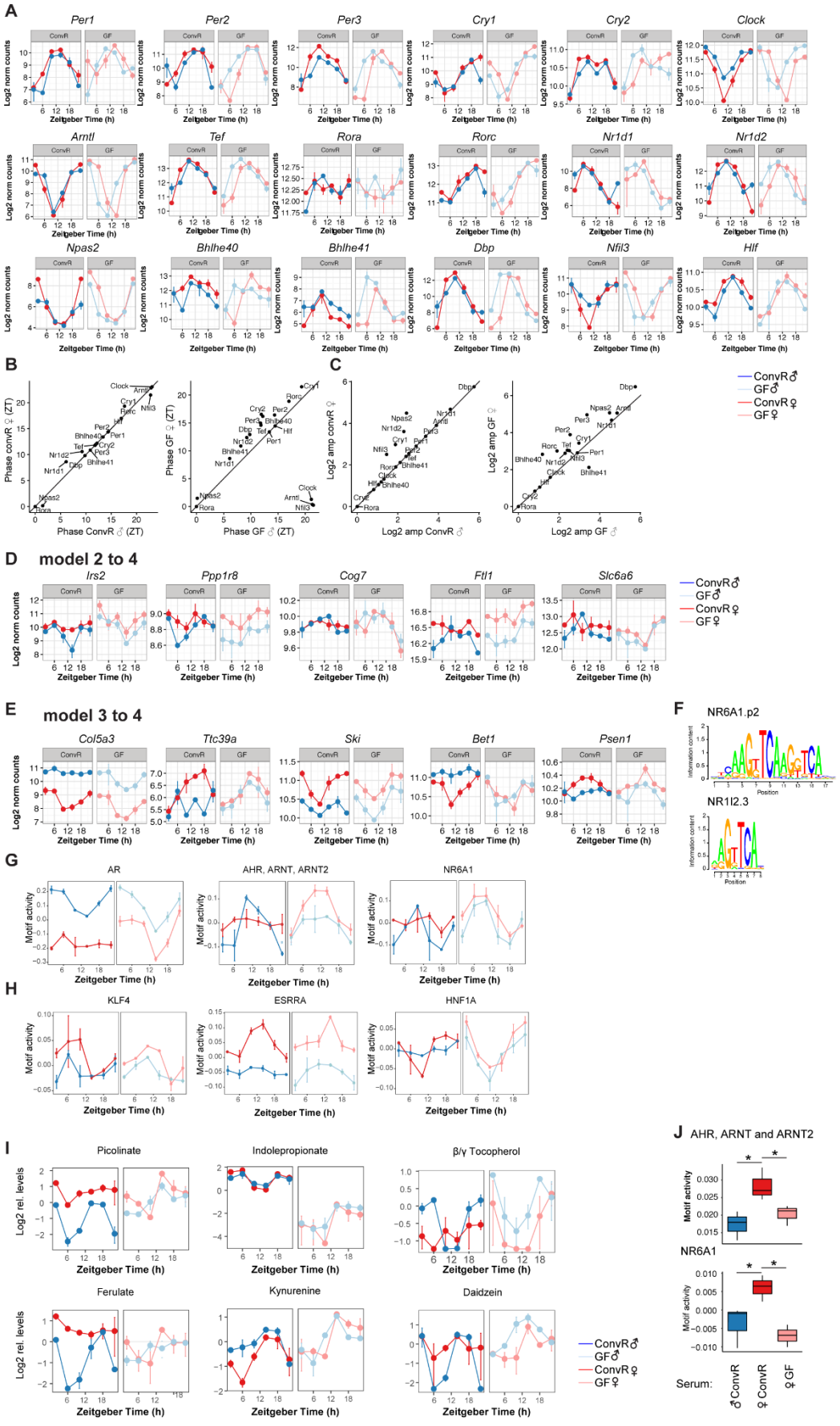

A. Hepatic clock gene expression data of male and female ConvR (ConvR♂, dark blue; ConvR♀, dark red) and GF (GF♂, light blue and GF♂, light red) animals.
B. Phase distribution of ConvR♂ and ConvR♀ (left) and GF♂ and GF♀ (right) of hepatic clock gene expression.
C. Amplitude comparison between ConvR♂ and ConvR♀ (left) and GF♂ and GF♀ (right) of clock gene expression in liver.
D, E. Selected temporal expression profile of genes that show male-specific (D) and female-specific (E) rhythmicity in ConvR animals that lose sex specific rhythmicity in the absence of microbiota.
F. Sequence logos of positional weight matrices (PWM) for NR6A1.p2 and NR1I2.3 used in the motif activity analysis reveals high similarity between the PWMs.
G,H. Temporal profiles of predicted activity for selected transcription factors that present a male- (G) or female-specific (H) rhythmic activity in ConvR that is not sex-specific in GF condition.
I. Temporal profile of metabolite levels for the indicated sex and hygiene status.
J. Predicted motif activity of indicated transcription factors in female hepatocytes treated with serum of ConvR♂, ConvR♀ and GF♀ mice. *, $p \leq 0.05$. Tukey boxplots represent three biological replicates. Error bars represent SEM.

Figure S6: Effects of late conventionalization and antibiotic treatment on sexually dimorphic hepatic gene expression and activation of xenobiotic receptors, related to Fig 6

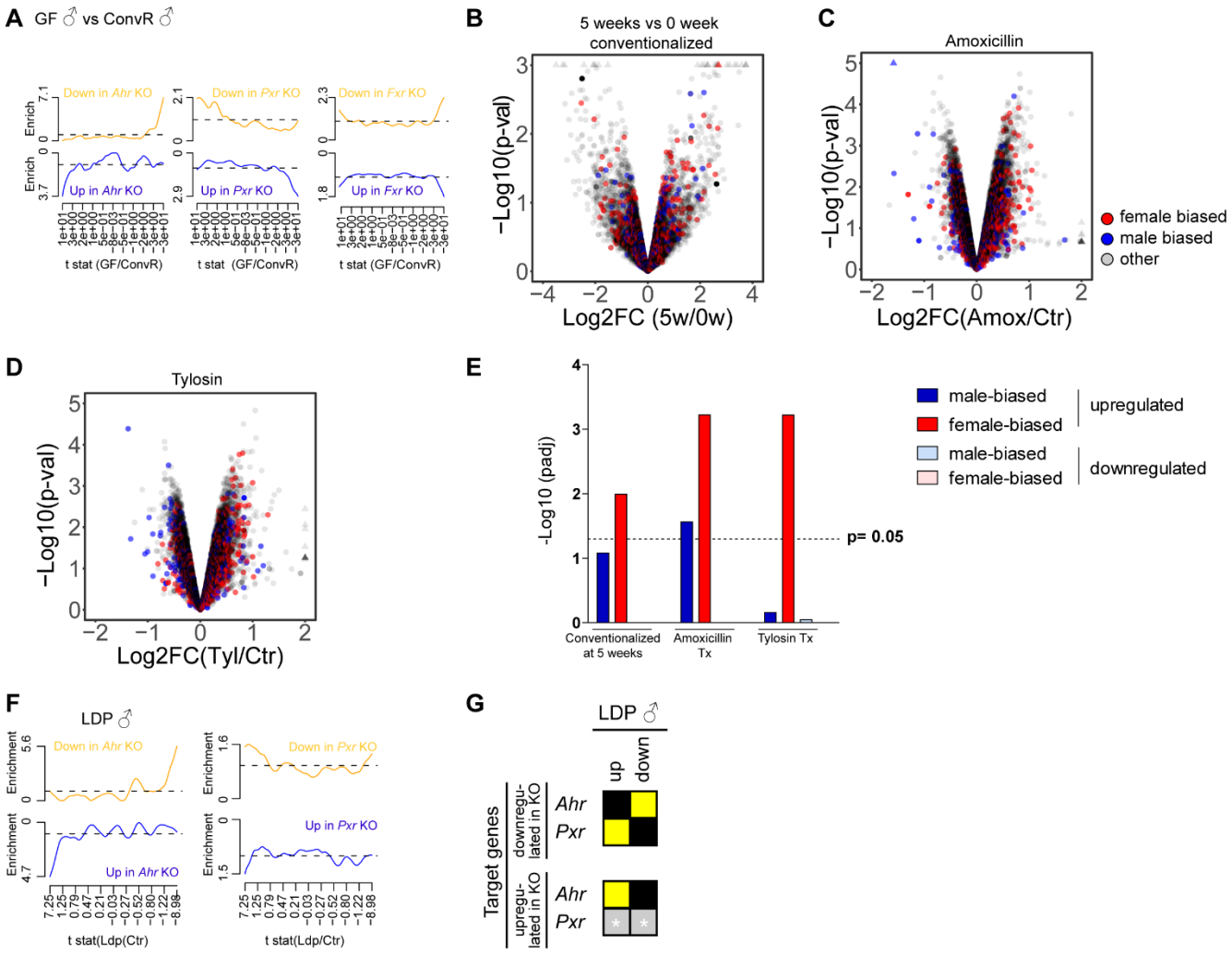

A. Enrichment for genes up- and down-regulated in *Ahr*, *Pxr* and *Fxr* KO animals in GF male animals. Genes are ordered by t-statistics from most up to most downregulated genes in the liver of GF♂ vs ConvR♂ mice. Relative enrichment of differentially expressed genes in the indicated KO are represented as an orange (upregulated in KO vs WT) or blue lines (downregulated in KO vs WT).

B-D. Changes in hepatic gene expression (log2FC) and p-values upon conventionalization of GF mice at 5 weeks of age compared to conventionalization at birth (B), amoxicillin (C) and tylosin treatment (D) of conventionally mice plotted as a volcano plot.

E. Associated p-values for significant enrichment of female-biased and male-biased genes in the subset of up- and down-regulated genes in the different conditions shown in panel B-D.

F. Enrichment for genes up- and down-regulated in *Ahr* and *Pxr* KO animals in low dose pencillin (LDP) treated animals. Genes are ordered by t-statistics from most up to most downregulated genes in the liver of LDP treated male mice. Relative enrichment of differentially expressed genes in the indicated KO are represented as an orange (upregulated in KO vs WT) or blue lines (downregulated in KO vs WT).

G. Heatmap summarizing the adjusted p-values for statistical enrichment analysis for genes with altered expression in *Ahr* and *Pxr* KO in the conditions represented in panel F.

Figure S7: Clock depletion affects sexually dimorphic hepatic gene expression, related to Fig 7

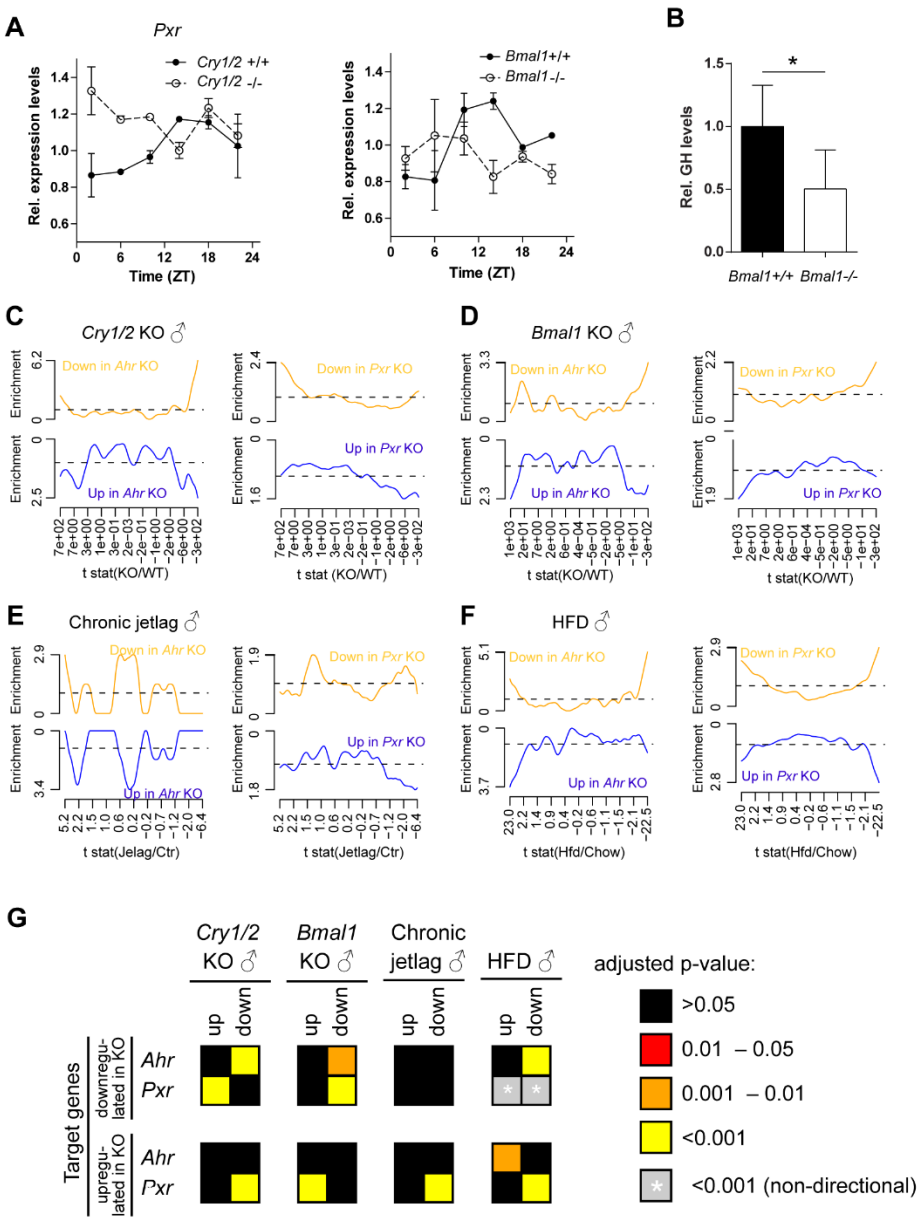

A. Rhythmic expression profile of *Pxr* in the liver of *Bmal1* and *Cry1*/*Cry2* KO mice. Each time point represents two independent biological replicates per condition.
B. *Bmal*1 KO show lower GH levels than their WT counterparts. Each bar represents 68 animals, error bar shows SEM. *, p<0.05, Mann–Whitney U test.
C-F. Enrichment for genes with altered expression in the liver of *Ahr* (left) and *Pxr* KO (right) mice for several contrasts: ConvR♂ animals on male *Cry1*/*Cry2* KO *vs* WT (C), male *Bmal1* KO *vs* WT (D), male chronically jetlagged (E), and ConvR♂ animals on HFD (F). Genes are ordered by t-statistics from most up to most downregulated genes of the corresponding contrast. Relative enrichment for differentially expressed genes in *Ahr* or *Pxr* KO are represented as orange (upregulated in *Ahr* or *Pxr* KO *vs* WT) or blue lines (downregulated in *Ahr* or *Pxr* KO *vs* wild-type).
G. Heatmap summarizing the adjusted p-values for statistical enrichment analysis for genes with altered expression in *Ahr* and *Pxr* KO in the conditions represented in panel C-F. Error bars represent SEM.